The role of gap junctions in transmitting electrical signals between cells

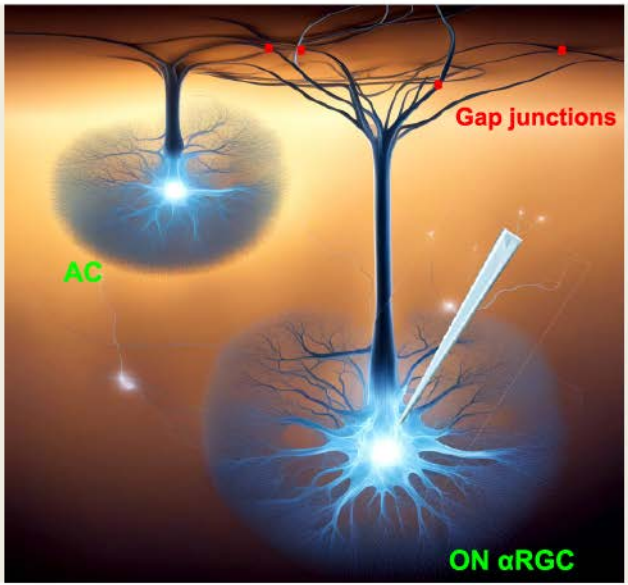

Bidirectional signaling occurs between coupled ACs and ON α-RGC through gap junctions.

AMERICAN JOURNAL OF PHYSIOLOGY
CELL PHYSIOLOGY.

american physiological society

Am J Physiol Cell Physiol 327: C716–C727, 2024.
First published July 16, 2024; doi:10.1152/ajpcell.00238.2024

american physiological society

AMERICAN JOURNAL OF PHYSIOLOGY
CELL PHYSIOLOGY

RESEARCH ARTICLE

Cell firing between ON alpha retinal ganglion cells and coupled amacrine cells in the mouse retina

Qin Wang,[1,2,4] ChungHim So,[1] and Feng Pan[1,2,3]

[1]*School of Optometry, The Hong Kong Polytechnic University, Kowloon, Hong Kong, People's Republic of China;* [2]*Centre for Eye and Vision Research (CEVR), 17W Hong Kong Science Park, Hong Kong, China;* [3]*Hong Kong Polytechnic University Shenzhen Research Institute, Shenzhen, Guangdong, People's Republic of China; and* [4]*University of Health and Rehabilitation Sciences, No. 369 Qingdao National High-Tech Industrial Development Zone, Shandong, People's Republic of China*

Abstract

Gap junctions are channels that allow for direct transmission of electrical signals between cells. However, the ability of one cell to be impacted or controlled by other cells through gap junctions remains unclear. In this study, heterocellular coupling between ON α retinal ganglion cells (α-RGCs) and displaced amacrine cells (ACs) in the mouse retina was used as a model. The impact of the extent of coupling of interconnected ACs on the synchronized firing between coupled ON α-RGC-AC pair was investigated using the dopamine 1 receptor (D1R) antagonist—SCH23390 and agonist—SKF38393. It was observed that the synchronized firing between the ON α-RGC-ACs pairs was increased by the D1R antagonist SCH23390, whereas it was eradicated by the agonist SKF38393. Subsequently, the signaling drive was investigated by infecting coupled ON α-RGC-AC pairs with the channelrhodopsin-2(ChR2) mutation L132C engineered to enhance light sensitivities. The results demonstrated that the spikes of ON α-RGCs (without ChR2) could be triggered by ACs (with ChR2) through the gap junction, and vice versa. Furthermore, it was observed that ON α-RGCs stimulated with 3–10 Hz currents by whole cell patch could elicit synchronous spikes in the coupled ACs, and vice versa. This provided direct evidence that the firing of one cell could be influenced by another cell through gap junctions. However, this phenomenon was not observed between OFF α-RGC pairs. The study implied that the synchronized firing between ON α-RGC-AC pairs could potentially be affected by the coupling of interconnected ACs. Additionally, one cell type could selectively control the firing of another cell type, thereby forcefully transmitting information. The key role of gap junctions in synchronizing firing and driving cells between α-RGCs and coupled ACs in the mouse retina was highlighted.

NEW & NOTEWORTHY This study investigates the role of gap junctions in transmitting electrical signals between cells and their potential for cell control. Using ON α retinal ganglion cells (α-RGCs) and amacrine cells (ACs) in the mouse retina, the researchers find that the extent of coupling between ACs affects synchronized firing. Bidirectional signaling occurs between ACs and ON α-RGCs through gap junctions.

amacrine cells; channelrhodopsin; gap junctions; retina; retinal ganglion cells

INTRODUCTION

Visual signaling in the retina is transmitted by both chemical and electrical synapses, also known as gap junctions (1). Gap junctions are cell-to-cell communication that allows ions and small molecules to pass directly from one cell to another, playing crucial roles in many physiological processes, such as signal averaging, synchronization, and noise reduction (2). However, it remains uncertain whether one cell can affect or even control the activities of other cells via gap junctions. The retina, part of the central nervous system (CNS), is an excellent model for studying the role of gap junction due to its easy accessibility for recording and well-understood circuitry.

The retina conveys visual information to the brain via retinal ganglion cells (RGCs) (3–6). Approximately 40 subtypes of RGCs encode different aspects of the visual scene in a parallel way (7–9). Alpha (α) RGCs, which are identifiable and recordable due to their large, broad dendritic fields and ON and OFF responses to visual stimuli, are arranged in a mosaic-like pattern across mammalian species (10, 11). These characteristics make α-RGCs a subject of interest for investigation. RGCs and amacrine cells (ACs) are crucial for visual processing, with ACs acting as interneurons that influence the activity of RGCs.

Furthermore, both ON α-RGCs and coupled displaced ACs, located on the surface of the RGC layer, provide an excellent opportunity to examine cell driving between them and the impact of the interconnected ACs network via gap junction on their synchronous firing. This also makes patch recording easier to perform. Therefore, understanding the interaction

Correspondence: F. Pan (feng.a.pan@polyu.edu.hk).
Submitted 11 April 2024 / Revised 26 June 2024 / Accepted 9 July 2024

between ON α-RGCs and coupled ACs can provide valuable insights into visual information processing and how various factors influence it.

Synchronized firing, facilitated by gap junctions in the CNS, plays an important role in neural coding by transmitting more information than single-neuron activity (12–16). In the visual system, it is believed that gap junctions between RGCs and ACs are responsible for the observed synchronized firing in these cells (17, 18), which is thought to enable the transmission of precise information related to stimuli (19, 20). ACs influence the encoding and conversion of visual input into electrical activity in RGCs. The strength of the coupling between inhibitory interneurons, specifically ACs, is known to affect the spatial coverage of RGCs. However, the extent to which coupled networks of ACs modulate the activity of RGCs in the retina is largely unknown. For instance, AC-AC coupling determines the spatial extent of the local luminance subtracted from the RGCs. It has also been proposed that the extent of AC-RGC coupling could determine how much the weight of the average contrast would affect the activity of RGCs (21). This study first aims to understand the influence of interconnected ACs coupling on pairing coupled ACs and ON α-RGCs. A study by Mills et al. (22) found that the permeability of gap junctions between ACs can be selectively reduced by a dopamine 1 (D1) receptor agonist (SKF38393), whereas the permeability between RGCs can be reduced by a dopamine 2 (D2) receptor agonist (quinpirole). Thus, the relative importance of the extent of coupling of ACs can be assessed using dopamine agonists, although it remains challenging to modulate the gap junctions between α-RGC and coupled ACs independently.

Cell driving or entrainment, which synchronizes one or more oscillating systems to an external rhythm, is a phenomenon widely observed across various physiological systems (23). This research also explored the potential mechanism of entrainment of activities between heterologous-coupled ACs and ON α-RGCs, as a model of different cell types.

Channelrhodopsin (ChR)-based microbial opsins, such as channelrhodopsin-2 (ChR2), are a commonly used optogenetic tool for genetically encoding light-gated channels (24). However, their application has been limited due to their low light sensitivity (25). Mutants of ChR2 at T159C and L132C have been discovered to increase light sensitivity and produce a larger current amplitude that is 1.5 log units lower than the wild-type (WT) ChR2 (26). The research used adeno-associated virus (AAV) vectors to introduce ChR2 mutations into retinal neurons. The ChR-infected cells were then used to test cell drive firing between ON α-RGCs and coupled ACs.

This study also examined whether RGCs could directly drive coupled ACs in the retinal network or vice versa. Depolarization waves were rhythmically injected from coupled cells to demonstrate the potential for one cell to drive the firing of another coupled cell. The possible driver direction between ON α-RGCs and coupled ACs was tested. In addition, the OFF α-RGCs pair was tested as a model of homocellular coupling for cell drive.

Our study showed that coupling networks of ACs can influence the activity of RGCs. ON α-RGCs and coupled displaced ACs can drive the spikes of each other, but not between OFF α-RGCs pairs. Gap junctions were essential for synchronous firing and cell driving between ON α-RGCs and coupled ACs in the mouse retina.

METHODS

Ethics Approval

All animal procedures were approved by the Animal Subjects Ethics Sub-Committee of the Hong Kong Polytechnic University (Approval No. 17-18/66-SO-R-GRF). All experiments complied with the *Guide for the Care and Use of Laboratory Animals* published by the National Institutes of Health.

Animals

Adult mice (*postnatal day 16–56*) C57BL/6J (RRID: IMSR_JAX:000664) wild-type (WT), $n = 59$, and Kcng4-YFP (6–8 wk, $n = 11$) mice (27), with labeled α-RGC, of either sex were used in the study.

DNA and Viral Vector Constructs

The single ChR2 mutations at the L132 sites, kindly provided by Dr. Zhuo-Hua Pan, were created by gene synthesis (GenScript, Piscataway, NJ). rAAV2 vectors carrying a fusion construct of ChR2 and green fluorescent protein (GFP), (ChR2-GFP), were driven by a cytomegalovirus (CMV) early enhancer/chicken β actin (CAG) hybrid promoter. The virus vectors were packaged and affinity purified at the Gene Therapy Program of the University of Pennsylvania or Virovek (Hayward, CA) (26).

Viral Vector Injection

To establish the expression of ChR2 channels in retinal neurons, injections of the virus vectors were administered to adult C57BL/6J mice and Kcng4-YFP mice. In brief, the animals were anesthetized via an intraperitoneal injection of a mixture of 120 mg/kg ketamine and 15 mg/kg xylazine. A small perforation was made under a dissecting microscope in the temporal scleral region with a sharp needle, and 1.5 μL viral vectors, diluted in saline at a titer of 5×10^{12} vector genomes per milliliter (vg/mL), or vehicle (saline), were injected into the intravitreal space through the perforation with a 32-gauge blunt Hamilton syringe. Both eyes of each animal were injected. After the injection, animals were kept on a 12-h:12-h light/dark cycle for 5 days before being euthanized for electrophysiological recordings.

Flattened Retina-Sclera Preparation

All experiments were performed during daylight hours. The mice were anesthetized deeply with an intraperitoneal injection of ketamine and xylazine (80 and 10 mg/kg of body weight, respectively), and lidocaine hydrochloride (20 mg/mL) was applied locally to the eyelids and surrounding tissues. Eyes were removed under dim red illumination and hemisected anterior to the ora serrata. The anterior optical structures and the vitreous humor were removed, and the resultant retina-eyecup with sclera attached, either whole or in sections, was placed in a superfusion chamber. Retinas were dissected into four equal quadrants for patch recordings and attached to a modified translucent Millicell filter ring (Millipore, Bedford,

MA). The flattened retinas were superfused with oxygenated mammalian Ringer's solution, pH 7.4, at 32°C (28). The anesthetized animals were killed by cervical dislocation immediately after enucleation.

Electrical Recording

Extracellular recordings were obtained from RGCs of eight WT mice in all retinal quadrants. Whole cell recordings were performed using an MultiClamp 700B amplifier connected to a Digidata 1550B interface and pCLAMP 10 software (Molecular Devices). Cells were visualized with near-infrared light (>775 nm) at ×40 magnification with a Nuvicon tube camera (Dage-MTI, Michigan City, IN) and differential interference optics on a fixed-stage microscope (Eclipse FN1; Nikon, Tokyo, Japan). Retinas were superfused at a rate of 1–1.5 mL/min with Ringers solution, composed of (in mM) 120 NaCl, 2.5 KCl, 25 $NaHCO_3$, 0.8 Na_2HPO_4, 0.1 NaH_2PO_4, 1 $MgCl_2$, 2 $CaCl_2$, and 5 D-glucose. The bath solution was continuously bubbled with 95% O_2-5%CO_2 at 32°C (29).

Dopamine receptor (D1R) agonist (SKF38393, [(±)-1-phenyl-2,3,4,5-tetrahydro-(1*H*)-3-(1*H*)-3-benzazepine-7,8-diol hydrobromide], 10 μM; Tocris, Ellisville, MO) or antagonist (SCH23390, [*R*(+)-7-chloro-8-hydroxy-3-methyl-1-phenyl-2,3,4,5-tetrahydro-1*H*-3-benzazepine hydrochloride] at low concentrations 5 μM, Sigma-Aldrich, St. Louis, MO; D-054) was applied to change the coupling of amacrine cells (1, 30). Cocktail application (50 μM MK-801, 10 μM CNQX [6-Cyano-7-nitroquinoxaline-2,3-dione, Sigma-Aldrich, St. Louis, MO; C239], 50 μM PTX [Picrotoxin, Sigma-Aldrich; P1675], 5 μM STR [Strychnine, Sigma-Aldrich; S8753], and 50 μM APB [L-(+)-2-Amino-4-phosphonobutyric acid], Sigma-Aldrich; A7929) was used to block chemical neurotransmission in the retina. The pharmacology experiments were performed under dim white room lights, with ~1.27×10^3 photons/μm^2/s measured at the location.

Electrodes were pulled to 5–7 MΩ resistance, with internal solutions consisting of (in mM) 120 potassium gluconate, 12 KCl, 1 $MgCl_2$, 5 EGTA, 0.5 $CaCl_2$, and 10 HEPES (pH adjusted to 7.4 with KOH). This internal solution was used in experiments in which spiking was not blocked. The liquid junction potential was estimated to be ~11 mV and was subtracted from the holding membrane potential. Spike trains were recorded digitally at a sampling rate of 10 kHz with Axoscope software sorted using Off-line Sorter (Plexon, Dallas, TX), NeuroExplorer (Nex Technologies, Littleton, MA) software.

The cross-correlation function (CCF) between two spike trains was obtained by measuring the time differences between spikes from one cell and spikes from the other cell. The significance of the results was assessed using 99% confidence limits. The cross-correlation curves were fit by the Gaussian functions with Origin software (Microcal, Northampton, MA) as follows:

$$y = y_0 + Ae^{-\left((x-x_0)^2\right)/(2w^2)}$$

where A is amplitude, and w is width.

To isolate the components of neuronal interaction in cross-correlation functions from those influenced by the coactivation of cells due to light stimulus, a shift predictor correction procedure was used for light-evoked activity. The shift predictor was created by offsetting one spike train over one or more stimulus intervals, using the same methodology as a regular cross-correlation function. The shift predictor was generated as the average of all possible interval shifts. A shift-predicted function was obtained by subtracting the shift predictor from the original cross-correlation function, which specifically captured correlations independent of the light stimulus. This procedure allowed for separating neuronal interactions from the effects of the light stimulus.

Dye Injection of ON and OFF α-RGCs and Their Coupled Amacrine Cells

The GFP-labeled cells were visualized at ×40 magnification, as described earlier, and were impaled under visual control using pipette tips filled with 4% Neurobiotin (Vector Laboratories, Burlingame, CA) and 0.5% Lucifer Yellow (Molecular Probes, Eugene, OR) in double-distilled water and then backfilled with 3 M KCl. The electrode resistance was ~100 MΩ. The impaled cells were then subjected to a biphasic current (+1.0 nA, 3 Hz). Afterward, the retinal pieces were fixed in 4% paraformaldehyde for at least 10 min. The tissues were incubated overnight at 4°C in 0.1 M phosphate buffer with 0.5% Triton-X 100 and 0.1% NaN_3 containing 1% donkey serum and then incubated after extensive washing Alexa-488 conjugated streptavidin (Invitrogen, Carlsbad, CA) 1:200 overnight at 4°C. The tissues were then mounted in Vectashield (Vector Laboratories) for observation.

To identify the coupled ON α-RGCs and displaced ACs in the living tissue, PoPro1 (P3581, Thermo Fisher Scientific, Waltham, MA), a fluorescent gap junction-permeant tracer, was used. By injecting RGCs along with PoPro1 with Alex 594, it is possible to recognize ON α-RGCs and ACs coupling in WT mouse retina. To further confirm the coupled ACs, Neurobiotin can then be injected to study the cells that show PoPro1 coupling (31). This method was used to stain RGC-AC pairs (32, 33).

Light Stimulation

A green (525 nm) light-emitting diode delivered uniform full-field visual stimulation on the retina's surface. The intensity of the square-wave light stimuli was calibrated with a portable radiometer/photometer (Ealing Electro-Optics, Holliston, MA) and expressed in terms of the time-averaged rate of photoisomerizations per rod per second (Rh*/rod/s). Light intensities were calculated assuming an average rod density of 437,000 rods/mm (34) and quantum efficiency of 0.67 (35). Blue light stimuli (460 nm) were generated by Mightex 1000 LED Drivers to focally illuminate cells (50 μm diameter) in transgenic mice expressing channelrhodopsin-2 (ChR2). The light intensity was adjusted to an average of 3.05×10^5 Rh*/rod/s.

Immunocytochemistry

After 4% formaldehyde fixation for 15 min, the tissues were rinsed extensively with 0.1 M phosphate buffer (PB), pH 7.4, before blocking with 3% donkey serum in 0.1 M PB with 0.5% Triton-X 100 and 0.1% NaN_3 overnight. The tissues were then incubated for 3–7 days at 4°C with the primary antibodies (goat anti-ChAT, 1:100; Millipore Cat. No. AB144P, RRID: AB_2079751) diluted in 0.1 M PB with 0.5% Triton-X100 and 0.1% NaN3 containing 1% donkey serum (36). After extensive washing, they were incubated in secondary antibodies [donkey anti-goat Cy-5 (1:200); Jackson ImmunoResearch Laboratories,

West Grove, PA], overnight at 4°C. After washing with 0.1 M PB, the tissues were mounted in Vectashield (Vector Laboratories) for observation. Neurobiotin was visualized with Cy3-conjugated streptavidin (Jackson ImmunoResearch Laboratories, West Grove, PA).

Imaging and Data Quantification

Images of whole retinal mounts were acquired on a ZEISS LSM 800 with an Airyscan (Zeiss, Thornwood, NY) confocal microscope using a ×43 objective [numerical aperture (NA) 1.3]. The instrument's XY resolution was 120 nm and 350 nm in z resolution, and all three channels were superimposed. *Z*-axis steps were usually 0.35 μm. Unless otherwise indicated, the resulting data are presented as means ± standard error of the mean (SEM).

Statistical analyses were performed using Origin software (OriginLab, Northampton, MA) and SPSS Version 25 (IBM, Armonk, NY). Statistically significant differences ($P < 0.05$) were determined using Student's *t* test.

RESULTS

Correlated Spiking between an ON α-RGC and a Coupled AC in the Mouse Retina

ON and OFF α-RGCs, labeled in the KCNG4-YFP mouse line, were used to determine synchronous activity patterns in the retinas. ON α-RGCs exhibit substantial RGC-AC coupling. Indirect electrical coupling between ON α-RGCs pairs can be achieved through gap junctions with multiple intermediary ACs (1). To verify the recorded cell pair was between an ON α-RGC and a coupled AC, an ON α-RGC (marked with weak yellow fluorescent protein, YFP) was injected with PoPro1 to visualize the coupled ACs (with a diameter of 2–5 μm). Subsequently, dye Alex 594 was injected into the RGC, and Neurobiotin was injected into the AC (shown with 488 fluorescence) to show the morphology (Fig. 1*A*).

Spontaneous spike trains were recorded from pairs of ON α-RGCs and coupled ACs using a loose-patch recording method. The cross-correlation function (CCF) was used to identify pairs of cells with the correlated activity that exceeded chance by fitting a Gaussian function to the data and observing histogram peaks above the 99% confidence level. The coordinated spontaneous spike activity can be observed between coupled ON α-RGCs and displaced AC (Fig. 1, *B* and *C*). The eight pairs of statistical significance are above the 99% confidence level. The single peak amplitudes (probability) are 0.25 ± 0.1 (means ± SEM), and the width of the single peak was 0.06 ± 0.01 s ($n = 8$, 8 of 10). Data were time-shuffled using a shift predictor protocol to display the spike correlations that were not time-locked to the light stimulus, which was then subtracted from the original CCF. Paired recordings from ON α-RGCs and coupled ACs showed that the spike synchrony was preserved (Fig. 1*D*). All eight pairs of the spike correlations disappeared after applying

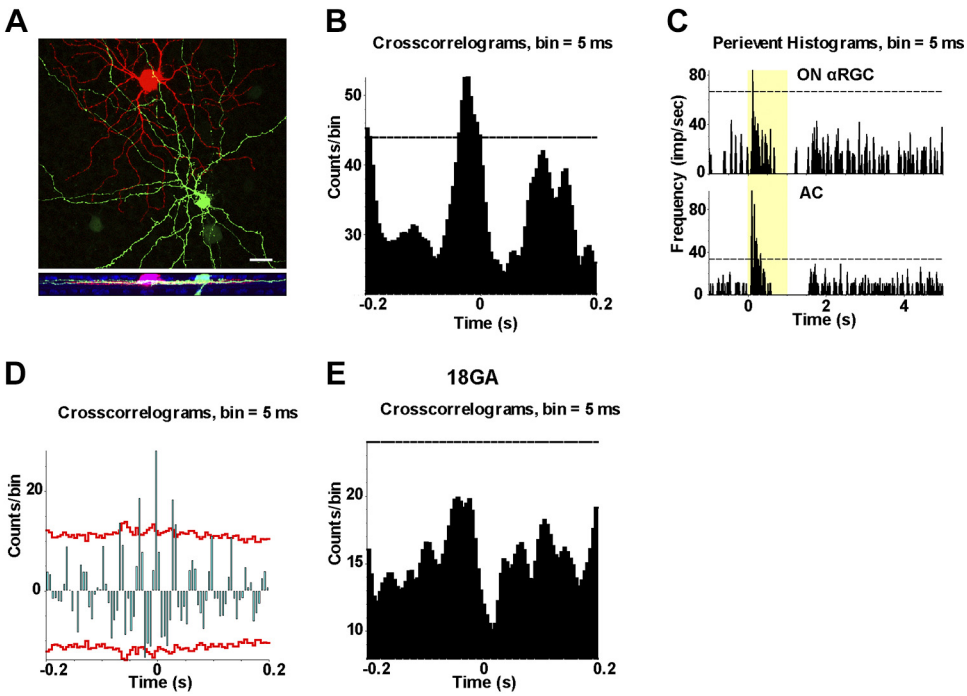

Figure 1. Synchronized firing pattern between coupled ON α-retinal ganglion cells (RGCs) and displaced amacrine cell (AC) in the mouse retina. *A*–*E*: a synchronized firing pattern between coupled ON α-RGCs and displaced AC (8 of 10 pairs). *A*: two neighboring ON α-RGCs and displaced AC visualized by 2 dye injections (Red-ON α-RGC with Alexa-594; Green-coupled displaced AC: Neurobiotin injection with 488 labeling). Triple labeled with anti-ChAT antibody (blue) showed the OFF sublaminar of the RGCs. Scale bar = 20 μm. *B*: cross-correlation functions (CCFs) of spontaneous spikes of the ON α-RGCs and coupled AC with a Gaussian function. CCFs produced a single peak model (width = 0.03 s). The ON α-RGCs are coupled with displaced AC. *C*: peristimulus time histograms (PSTHs) of 2 coupled ON α-RGCs and displaced AC responses. Presentation of the 525-nm full-field light stimulation, intensity = 131 Rh*/rod/s is indicated by the yellow bar. The dotted line represents the 99% confidence interval, above which correlations are above chance. *D*: shift predictor CCFs computed from the ON α-RGCs and coupled AC with common input showed coherent firing. The red line represents the 99% confidence interval, above which the correlations are above chance. *E*: blockage of gap junctions with 30 μm 18-β-glycyrrhetinic acid (18b-GA) effectively eliminated spike correlations.

gap junction blockers—30 μM 18-beta-glycyrrhetinic acid (18b-GA) (Fig. 1*E*), indicating that gap junctions were responsible for generating the synchronized spikes.

It is notable that the spontaneous firing rates of ON α-RGCs and displaced ACs exhibited significant variability, particularly under different lighting conditions. From these eight pairs, the spontaneous firing rates of ON-transient α-RGCs were recorded at 7.4 ± 3.0 Hz ($n = 5$), in contrast to 3.1 ± 1.8 Hz ($n = 3$) for ON-sustained α-RGCs. The data suggests that ON-transient α-RGCs have higher spontaneous firing rates than ON-sustained α-RGCs. The disparity in firing rates may be explained by the fact that transient and sustained ON α-RGCs are distinct subtypes of retinal ganglion cells, each forming unique connections with different ACs, which could lead to the observed differences in their synchronized spiking patterns. However, to fully understand these mechanisms, further experimental research is necessary.

The Influence of Amacrine Cell Coupling on Synchronized Firing between ON α-RGCs and Coupled ACs

The impacts of AC-AC coupling on the synchronized firing pattern of coupled pairs between ON α-RGCs and coupled ACs were tested. It was found that the synchronized firing between ON α-RGCs and displaced ACs (their statistical significance is above the 99% confidence level; the single-peak amplitudes (probability) are 0.2 ± 0.1, means ± SEM) was eliminated by applying 10 μM D1R agonist SKF38393 after 3 min ($n = 5$, 5 of 8) (Fig. 2, *A* and *C*). On the other hand, the application of D1R antagonist SCH2339 increased the synchronized firing of CCFs of spontaneous spikes of the ON α-RGCs and coupled displaced ACs in 1 min (after normalization, the single-peak amplitude increased from 0.22 ± 0.1 to 0.43 ± 0.1, means ± SEM; $n = 5$, 5 of 7) (Fig. 2, *D–H*). As the coupling of ACs increased, the synchronized cell firing pattern also altered, resulting in three peaks in 1 min (Fig. 2*F*), multiple peaks in 3 min (Fig. 2*G*) and 5 min (Fig. 2*H*). Over time, the spike frequency of the ON α-RGC-AC pairs also increased, suggesting that additional coupled ACs were participating in the synchronized firing of spontaneous spikes of the coupled ON α-RGC-ACs network. Specifically, multiple peaks in synchronized activity during the 3- to 5-min interval could suggest the involvement of 3–5 ACs coupled with a single ON α-RGC.

Cell Drive between Coupled ON α Retinal Ganglion Cells and Amacrine Cells

The study further explored whether one cell could stimulate or drive the spike in another coupled cell between the different cell types in the retina. The ON α-RGCs and the coupled ACs were tested as examples because the ON α-RGC and the coupled ACs are situated near the retina's surface, making a cell patch feasible.

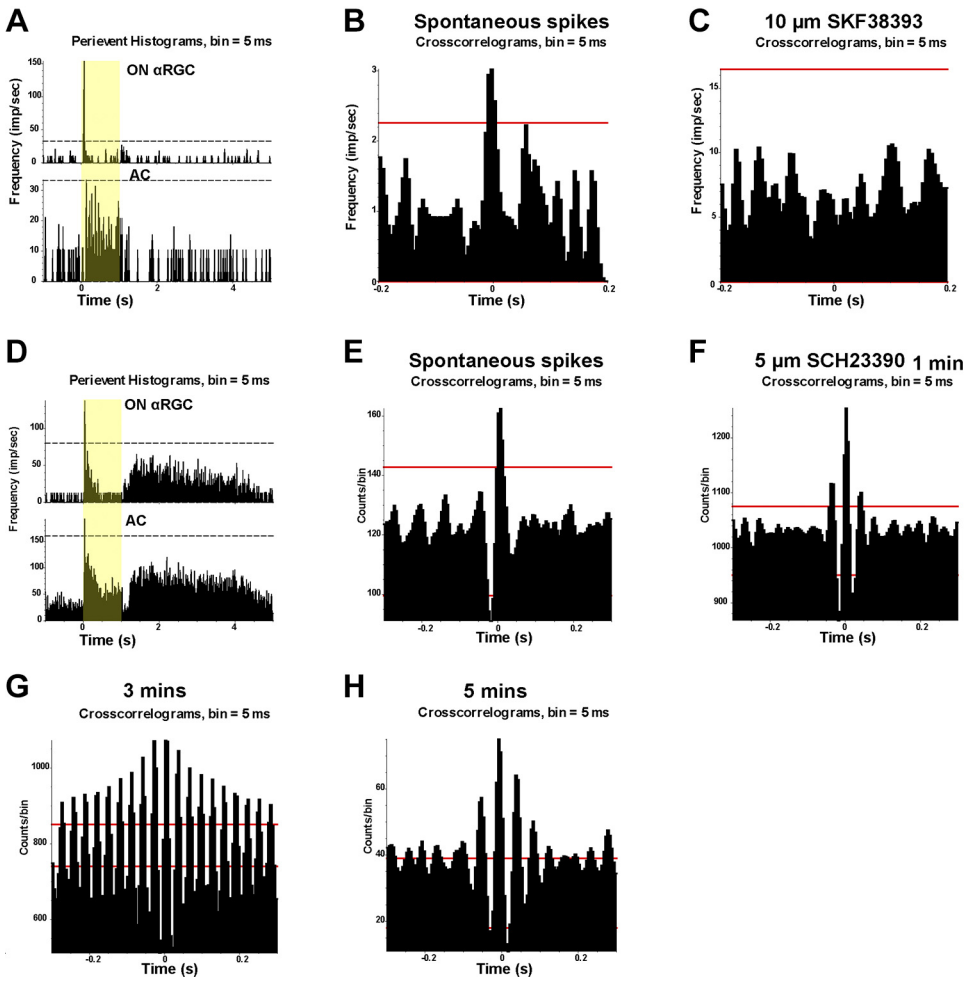

Figure 2. Dopamine 1 (D1) receptor agonist SKF38393 and antagonist SCH23390 on ON α-retinal ganglion cells (RGCs) and coupled amacrine cells (ACs). *A*: peristimulus time histograms (PSTHs) of neighboring ON α-RGCs and coupled AC responses. Presentation of the 525 nm full-field light stimulation, intensity = 131 Rh*/rod/s is indicated by the yellow bar. *B*: cross-correlation functions (CCFs) of spontaneous spikes of neighboring ON α-RGCs and coupled AC with a Gaussian function. CCFs display a single peak model (width = 0.03 s). *C*: 10 μM D1 receptor agonist SKF38393 will eliminate spike correlations after application. *D*: PSTHs of two neighboring ON α-RGCs and coupled AC responses. Presentation of the 525-nm full-field light stimulation, intensity = 131 Rh*/rod/s is indicated by the yellow bar. *E*: CCFs of spontaneous spikes of neighboring ON α-RGCs with a Gaussian function. CCFs display a single peak model (width = 0.03 s). *F–H*: 5 μm D1 receptor antagonist SCH23390 increased spike correlations from 1 to 5 min after application.

AJP-Cell Physiol • doi:10.1152/ajpcell.00238.2024 • www.ajpcell.org

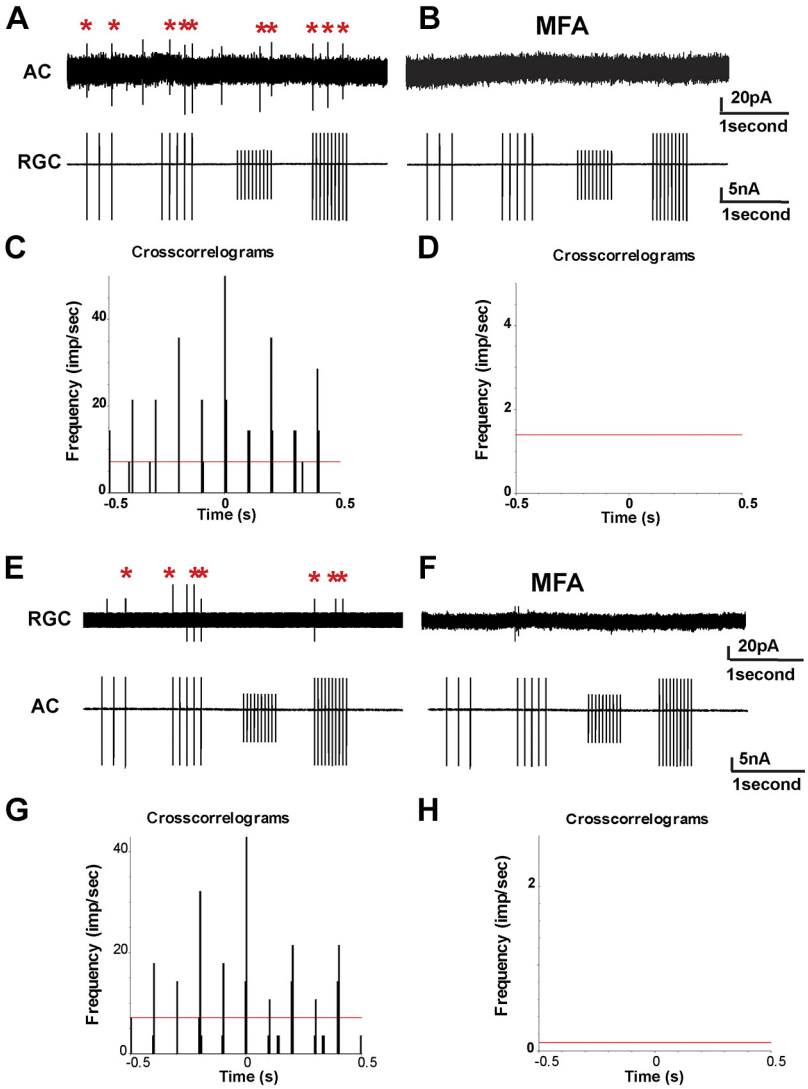

Figure 3. ON α-retinal ganglion cells (RGCs) and coupled amacrine cells (ACs) can drive the spikes to each other. *A*: coupled ON α-RGCs and nearby AC were recorded. The RGC with the whole cell patch was injected currents at 3 and 5 Hz with 10 nA followed by 10 Hz 5 nA and then 10 Hz 10 nA. The injected current could drive the spikes of coupled AC. The red star indicates the induced spikes. *B*: 50 μM meclofenamic acid (MFA) blocked the injected current from RGC to drive the spikes of coupled AC. *C*: the CCF is computed from cell-driven spikes recorded from the ON α-RGCs and coupled AC pair. The red line represents the 99% confidence limit, above which, correlations are above chance. *D*: the CCF showed no synchronous relationship between the ON α-RGCs and coupled AC after 50 μM MFA application to block the gap junction. *E*: coupled ON α-RGCs and nearby AC were recorded. The AC with the whole cell patch was injected currents at 3 and 5 Hz with 10 nA followed by 10 Hz 5 nA and 10 nA. The injected current could drive the spikes of coupled RGC. *F*: 50 μM MFA blocked the injected current from AC to drive the spikes of coupled RGC. *G*: the CCF is computed from cell-driven spikes recorded from the AC and coupled ON α-RGC pair. The red line represents the 99% confidence limit. *H*: the CCF showed no synchronous relationship between AC and coupled ON α-RGC.

An ON α-RGC was held with a whole cell patch and then injected with a serial burst of currents at 3 Hz and 5 Hz with 10 nA, followed by 10 Hz of 5 nA and 10 nA. The driving from ON α-RGCs induced the spikes of nearby ACs ($n = 6$, 6 of 8) (Fig. 3*A*). The CCF computed from the ON α-RGCs and ACs pair indicated a synchronous firing relationship (Fig. 3*C*). As confirmed by the CCF, a concentration of 50 μM meclofenamic acid (MFA) could block the current injected into the ON α-RGCs from driving spikes in the coupled ACs (Fig. 3, *B* and *D*). The injection of PoPro1 further confirmed the relationship between the ON α-RGCs and the coupled ACs.

Subsequently, to test whether ACs can drive the spikes of coupled RGCs, the nearby AC was patched and stimulated with a serial burst of currents at 3 Hz and 5 Hz with 10 nA, followed by 10 Hz of 5 nA and 10 nA ($n = 5$, 5 of 8) (Fig. 3*E*). This stimulation induced spikes in the coupled RGCs and drove their firing in a synchronous pattern (Fig. 3*G*). Similarly, 50 μM MFA also blocked the current injected into the AC from driving spikes in the coupled ON α-RGCs, as confirmed by the CCF (Fig. 3, *F* and *H*).

The frequency tested for cell drive was up to 900 Hz applied in the study. High-frequency (above 100 Hz) bursts of currents barely induce spikes in the coupled cell because the afterhyperpolarization controls the spike timing precision (37). The OFF RGC and coupled OFF RGC were also tested with one RGC patched with a whole cell patch and then stimulated with a serial burst of currents. However, no spikes could be induced in the couple of RGCs yet.

Expression and Light-Response Properties of ChR2 in ON α Retinal Ganglion Cells and Displaced Amacrine Cells

After an extended incubation period exceeding 10 days, cells expressing ChR2-GFP became visible throughout the inner nuclear layer, encompassing horizontal cells as well. In this experiment, GFP fluorescence was primarily seen in the RGC layer (Fig. 4*A*) 5 days after the viral vectors were injected into the intravitreal space, verifying the expression of ChR2-GFP.

To test the functional properties of the L132C in the OFF α-RGC layer, loose patch recordings were used to detect light-induced spikes to a full-field 460 nm light stimulus (1-s light intensity of 3.05×10^5 Rh*/rod/s) (Fig. 4*B*). This light was generated by Mightex 1000 LED Drivers to focally

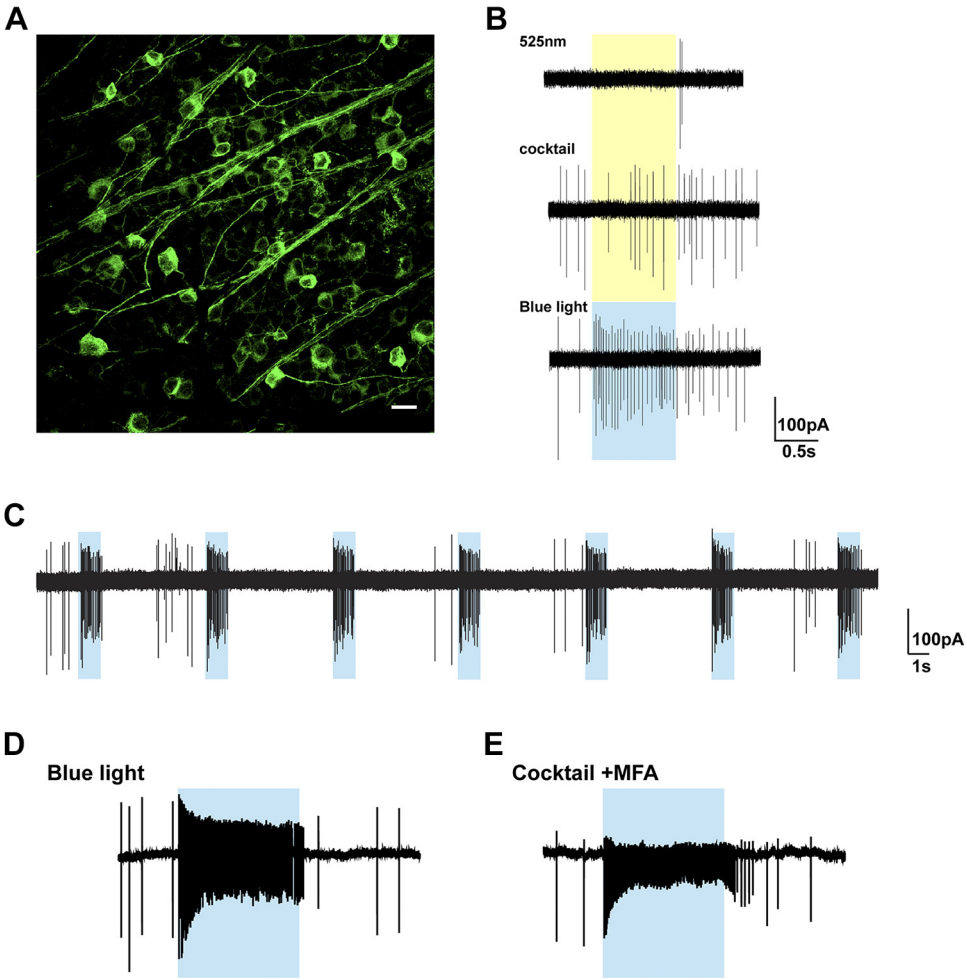

Figure 4. Alpha retinal ganglion cell (RGC) with channelrhodopsin-2- green fluorescent protein (ChR2-GFP) expression. *A*: fluorescence images of GFP expression for ChR2 mutants L132C in wild-type whole mount retina. *B*: an α-OFF RGC with ChR2-GFP expression targeted for spike recording. *Top*: spike response of the α-OFF RGC after a 1-s 525-nm full-field light stimulation (intensity = 1,131 Rh*/rod/s). *Middle*: the α-OFF RGC lost the light-evoked responses to the same light stimulation after cocktail application, but not spontaneous responses (50 μM MK-801, 10 μM CNQX, 50 μM PTX, 5 μM STR, and 50 μM APB). *Bottom*: the spike responses were elicited in ChR2-GFP expressing α-OFF RGC by a 1-s 460-nm full-field light stimulation (intensity = 113.1 Rh*/rod/s). *C*: the spike responses of the same ChR2-GFP expressing α-OFF RGC (460 nm full-field light stimulation with 1-s stimulation at 5-s interval intensity = 3.05×10^5 Rh*/rod/s) persisted without spike attenuation and decayed with light stimulation. *D*: the image shows the spike responses of the same ChR2-GFP expressing α-RGC (460 nm full-field light stimulation with 1-s stimulation at 5-s interval intensity =3.05×10^5 Rh*/rod/s). *E*: the light response after a cocktail and gap junction blocker meclofenamic acid (MFA) (50 μM) application.

illuminate the cell (50 μm diameter) centered in ChR2-GFP soma, so that the responses of the other nearby cells could be minimized. After blocking all excitatory and inhibitory chemical synapses with a cocktail solution (38), 460 nm wavelength light (light intensity 3.05×10^5 Rh*/rod/s) induced the strong ON spikes. These consistent and robust light responses persisted with repeated light stimuli (Fig. 4*C*). Strong spikes were still observed in the application of both cocktails for blocking chemical synapses and 50 μM MFA for blocking gap junctions (Fig. 4, *D* and *E*).

Synchronized Spiking of ChR2-Mediated Activities between ON α-RGCs and Coupled ACs

In this study, the retina was infected with a ChR2 (L132C)-AAV2 viral vector for 5 days. ON a RGC can couple to several ACs in different layers. The experiment focused on a pair of coupled ON α-RGC-ACs ($n = 4$), with only the displaced ACs expressing ChR2-GFP, to observe whether the spikes of one cell could influence the other. These pairs were somewhat difficult to find, but it was not an impossible task (Fig. 5, *A*–*F*).

Experiments were repeated using intense 525 and 460 nm blue light to activate photoreceptors, followed by applying gap junction blockers to determine the role of gap junctions in generating synchronized activity in response to light stimuli. In addition, the synchronized correlation between coupled displaced ACs (ChR2) pairs of ON α-RGCs will be examined using CCFs of spontaneous spiking and shift predictor. Initially, the direct-coupled ON α-RGCs (without ChR2) and displaced ACs (with ChR2) were tested under 1-s 525-nm light stimuli, which induced strong spikes in both cells (Fig. 6, *A* and *B*). Repeated 1-s 460-nm blue light also induces strong spikes from the same cell pair. Shift predictor CCFs computed from the pair of neighboring ON α-RGCs and displaced ACs in response to common input showed synchronized firing (Fig. 6, *C* and *D*). However, after applying the gap junction blocker 50 μM MFA, the displaced AC (with ChR2) maintained its light response, but the ON α-RGC (without ChR2) lost its light response (Fig. 6*E*). These four pairs of ON α-RGCs-AC show that correlated activity is evoked by a contiguous light stimulus, which is decreased significantly (Student *t* test; $P < 0.05$) from 0.4 ± 0.1 to 0.15 ± 0.1 (after normalization) by MFA application. Shift predictor CCFs computed spike frequency from the cell pair in response to common input decreased, yet still showed synchronized firing (Fig. 6*F*). This could be because no cocktail was applied, and the common input still existed.

To block responses from all photoreceptor pathways, direct-coupled ON α-RGCs (loaded with ChR2) and displaced ACs (without ChR2) were paired recording and confirmed with spontaneous spikes in darkness (Fig. 7*A*). Exposure to repeated 1-s 525 nm green light elicited light-evoked responses in the cell pair (Fig. 7*B*). However, these light-

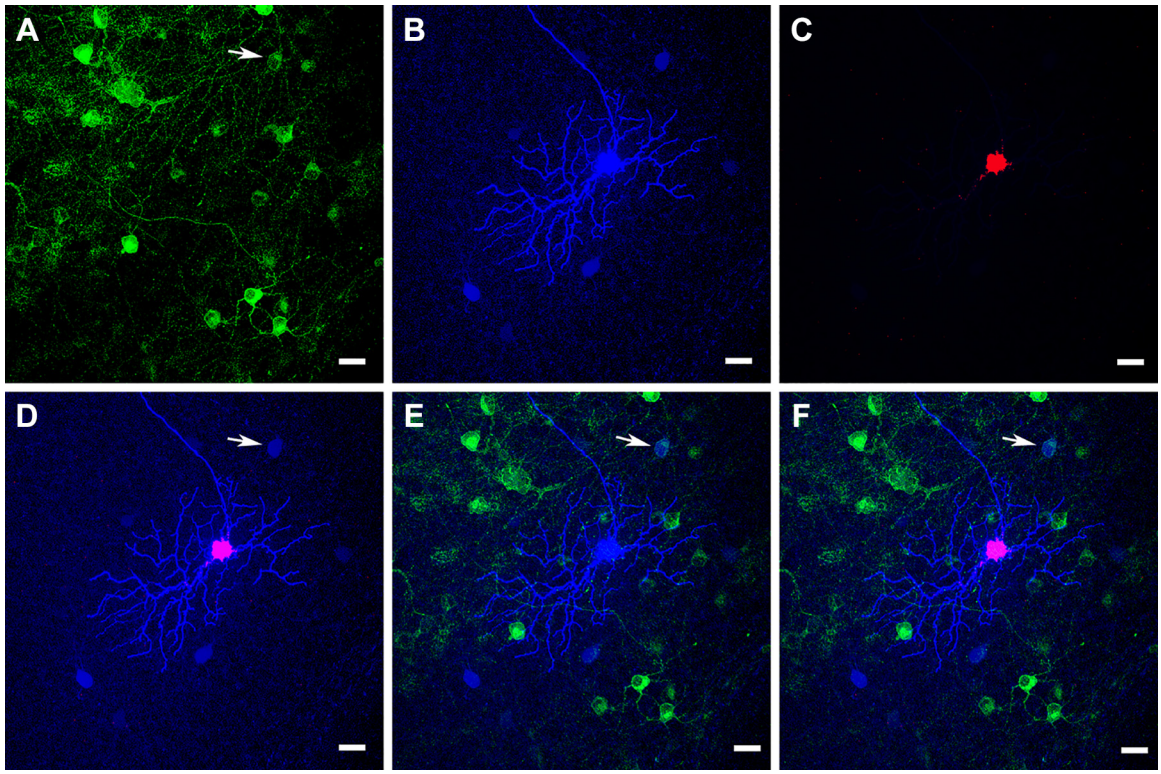

Figure 5. channelrhodopsin-2-green fluorescent protein (ChR2-GFP) expression displaced amacrine cell (AC) and coupled ON α-retinal ganglion cell (RGC) without ChR2. *A*: GFP-labeled cells with ChR2 mutants L132C in wild-type whole mount retina. Arrowhead indicates a displaced amacrine cell (AC). *B*: ON α-RGC and displaced ACs displayed with Neurobiotin injection (blue color of Alex 633). *C*: the recorded ON α-RGC soma was shown by Alex594 injection. *D*: Alex 594 shows ON α-RGC. Arrowhead indicates that a displaced AC is coupled with ON α-RGC. *E*: arrowhead shows the displaced AC also infected with AAV2-ChR2 (arrowhead). *F*: triple-labeled image shows the ON α-RGC and coupled AC.

evoked responses were eliminated upon administering the application of cocktail (50 μM MK-801, 10 μM CNQX, 50 μM PTX, 5 μM STR, and 50 μM APB) (Fig. 7*C*). Subsequently, repeated 1-s 460-nm blue light triggered robust light-evoked spikes in ON α-RGCs (with ChR2) and also induced the spike in the coupled ACs (without ChR2) (Fig. 7*D*). Nevertheless, after applying the gap junction blocker 50 μM MFA, the spikes in the coupled ACs were suppressed, whereas the ON α-RGCs (with ChR2) continued to respond (Fig. 7*E*).

DISCUSSION

Dopamine is released by a subset of amacrine cells and has widespread effects on various retinal neurons and circuits (39). Dopamine serves as a key modulator for adapting the retina to varying light conditions (1). Dopamine release increases in response to light, particularly during the transition from dark to light conditions, which suggests its involvement in the adaptation of the retina to bright environments.

One of the key functions of dopamine in the retina is to modulate the coupling between different types of retinal cells, including retinal ganglion cells (RGCs) and amacrine cells (ACs) (40). Gap junctions mediate this electrical coupling, which can synchronize their activity. These gap junctions are typically more conductive in the dark, leading to a higher degree of coupling and greater spatial summation and sensitivity to low light levels. Research indicates that dopamine can enhance or weaken the antagonistic surrounds of RGCs in a subtype-specific manner, affecting response kinetics and receptive field structure (41). In addition, dopamine has been found to influence the retinal clock mechanism during development, modulating the molecular core of the clock through melanopsin-dependent regulation of acetylcholine retinal waves (42). Moreover, dopamine levels in the retina have been linked to the development of myopia, with decreased dopamine levels associated with myopia progression (43). Overall, dopamine's multifaceted effects on the retina underscore its importance in visual signaling and retinal physiology.

Synchronized firing between coupled RGCs and ACs (17, 44) through gap junctions plays an important part in neural coding, allowing for the transfer of exact information related to stimulus patterns and position in the visual system (13, 19). Previous tracer coupling studies (45, 46) and research by the Bloomfield group (47–49) had demonstrated the essential role of gap junctions in producing synchronized firing. Nevertheless, the impact of interconnected ACs networks on ON α-RGCs and coupled ACs activity remains unexplored. This research used dopamine D1 antagonists and agonists, known to significantly impact AC-AC coupling (50, 51), to explore how the extent of interconnected ACs networks affects the spike coincidences of ON α-RGCs and coupled ACs. The D1 antagonist SCH-23390 or dim background light dramatically increases AC-AC coupling, whereas D1 agonist SKF 38393 or bright background light decreases AC-AC

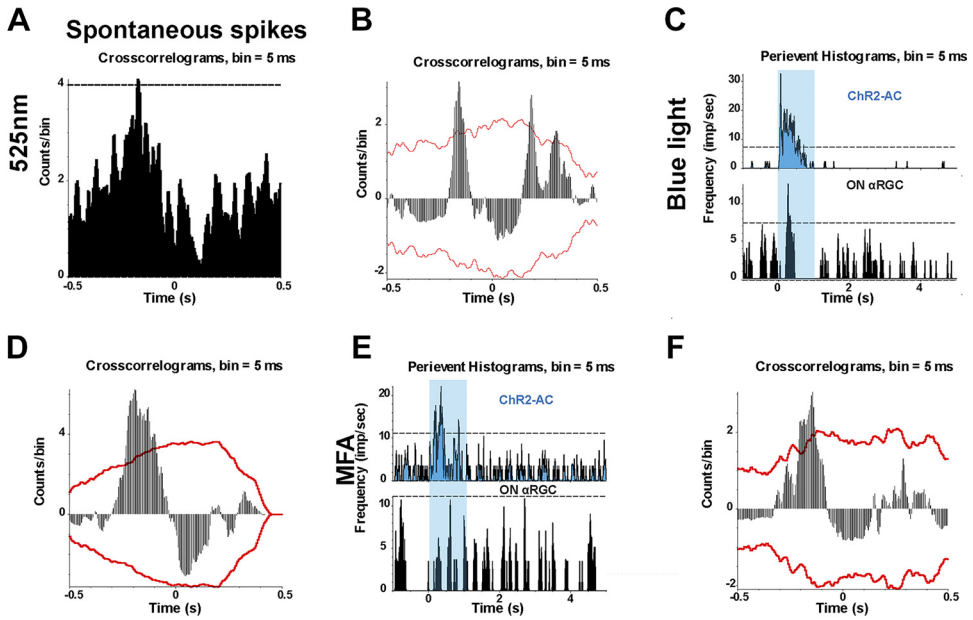

Figure 6. Synchronized firing between coupled ON α-retinal ganglion cell (RGC) and displaced amacrine cells (AC) (channelrhodopsin-2, ChR2). *A*: cross-correlation functions (CCFs) show spontaneous firing between ON α-RGC and a coupled displaced AC (ChR2) with coherent firing. *B*: shift predictor CCFs show that the pair of ON α-RGCs and AC had coherent firing under 525 nm light. Shift predictor CCF is a method designed to separate authentic neuronal interactions from correlations that arise due to light stimulation. It is accomplished by creating a shift predictor, which is done by shifting the spike train of one neuron by various stimulus intervals and calculating the average. This average is then subtracted from the original cross-correlation function to obtain a corrected function that accurately represents neuronal interactions, excluding the effects of the light stimulus. *C*: peristimulus time histograms (PSTHs) show spike responses to 1-s 460-nm light stimuli (intensity = 3.05×10^5 Rh*/rod/s) of the ON α-RGC (loaded with ChR2) and displaced AC. *D*: shift predictor CCFs show that the ON α-RGC and AC pair had a coherent firing under 460 nm. *E*: 50 μm meclofenamic acid (MFA) affected the spike responses of the pair of ON α-RGC and displaced AC. PSTHs show 50 μm MFA blocked ON α-RGC driving the firing of ChR2-labeled AC. *F*: shift predictor CCFs show pairing ON α-RGC and AC decreased coherent firing. The coherent firing may result from common input because the cocktail was not applied.

coupling (1, 22, 30). D1 antagonist increased the synchrony in pairs of ON α-RGCs with coupled ACs. Conversely, the D1 agonist diminished or eradicated synchrony.

Gap junctions between RGCs and ACs may help to filter and reduce temporal noise, thereby enhancing or decreasing the likelihood of firing in coupled RGCs and ACs for a brief period. This process can modulate the output signals of the RGCs to the brain (52–54). ACs provide feedback inhibition, surround inhibition, adaptation, signal averaging, and noise reduction (54, 55). They also help shape visual processing by

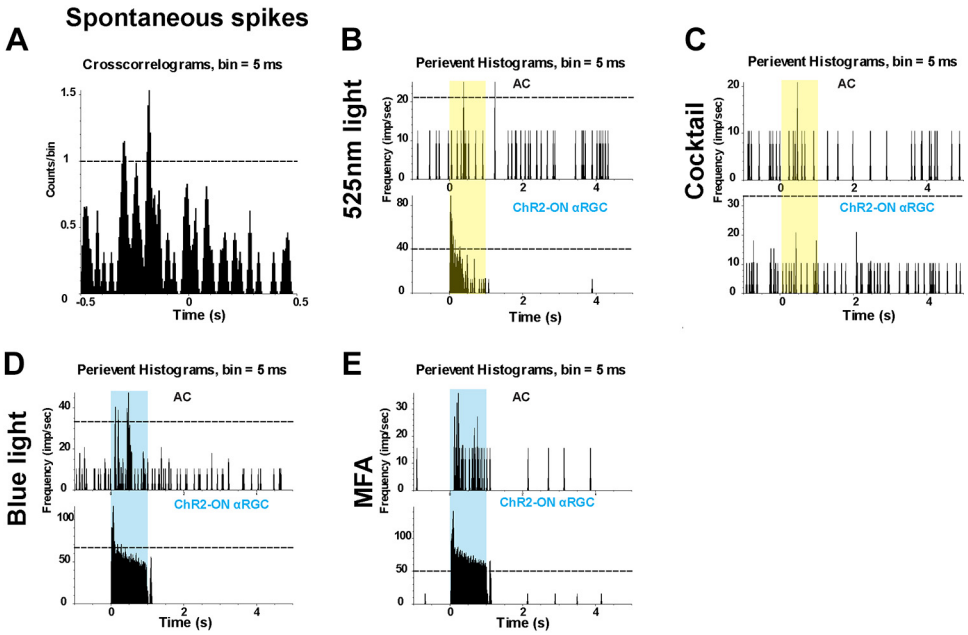

Figure 7. Synchronized firing between coupled ON α-retinal ganglion cell (RGC) [channelrhodopsin-2 (ChR2)] and displaced amacrine cell (AC). *A*: cross-correlation functions (CCFs) reveal spontaneous, synchronized firing between the ON α-RGC (ChR2) and a coupled displaced AC, indicating coherent firing patterns. *B*: peristimulus time histograms (PSTHs) show the light-evoked responses of the ON α-RGC (loaded with ChR2) and displaced AC to 1-s 525-nm full-field light stimulation at an intensity = 131 Rh*/rod/s. *C*: PSTHs illustrate the disappearance of light-evoked responses following the application of cocktail (50 μM MK-801, 10 μM CNQX, 50 μM PTX, 5 μM STR, and 50 μM APB) to block the chemical synaptic transmission. *D*: PSTHs show the light-evoked responses to 1-s 460 nm light stimuli (intensity = 3.05×10^5 Rh*/rod/s) in both the ON α-RGC (with ChR2) and displaced AC. *E*: the application of 50 μM meclofenamic acid (MFA) is shown to suppress the spike responses in the displaced AC, whereas the ON α-RGC (with ChR2) continues to exhibit light-evoked activity.

AJP-Cell Physiol • doi:10.1152/ajpcell.00238.2024 • www.ajpcell.org

computing local contrast in the circuit formed around each RGC type. RGCs are coupled to two to three types of ACs, each type of ACs potentially serving specific functions in visual processing (56, 57). The degree of AC-AC coupling could determine the spatial extent of local luminance to be subtracted from the RGCs (58). The extent of interconnected ACs coupling to RGCs could determine the impact of the average contrast when applied to RGCs (21). The physiological properties of many AC subtypes are not yet known, and only a few specific AC subtypes have been categorized in terms of their coupling partner(s) or particular function. Understanding the mechanisms leading to synchrony is crucial in disorders such as seizures, schizophrenia, epilepsy, autism, Alzheimer's disease, and Parkinson's disease (59).

Entrainment is a phenomenon observed in various physiological systems (60, 61). It involves adjusting the frequency and phase of firing in one cell by introducing periodic stimulation into adjacent coupled cells through local gap junctions (62). Gap junctions can also boost the probability of simultaneous spikes, while entrainment is the gradual effect of one cell's response by another, leading to an increased level of synchronous firing and patterning of spike trains. The most persuasive evidence for entrainment would come from showing frequency- and phase-locking dependencies between the two cells. Entrainment of one cell by another would result in a higher degree of correlated spikes than spikes produced by the two cells from other frequency or phase combinations, as all spikes would be adjusted to match each other in timing. Within the retina, the coupling between ON α-RGCs and ACs can be driven by each other at low frequency. High-frequency (above 100 Hz) bursts of currents barely induce spikes in the coupled cell, possibly due to the gap junction filtering the high frequency. Interestingly, an OFF α-RGC also cannot directly drive spiking in another OFF α-RGC that is directly coupled to it. This is likely due to the large soma of the OFF α-RGC, which requires a higher current to be driven. Another possible reason could be the extensive coupling of ACs with OFF RGCs. An OFF RGC is coupled to other OFF α-RGCs and ACs, which may affect the cell drive due to the difference in coupling patterns with ON α-RGC.

By introducing light-sensitive tools into RGCs or ACs using an optogenetic method, it is possible to manipulate neural circuitry (63). AAV2 vector-based ChR2 cells can facilitate firing between ON α-RGCs and coupled ACs through gap junctions. The study showed that 460-nm light stimulation could drive spikes in another coupled cell via the gap junction. However, the spikes produced through the stimulation of 460-nm light differ from those encountered in the natural environment due to the intense illumination of blue light applied. Research suggested that ON α-RGCs and ACs could drive the firing of each other. AC coupling could shape the information of ON α-RGCs during this transmission process.

The study implied one cell could impact or control the other cells through gap junctions. Gap junctions might play a key role in synchronizing firing and driving cells between ON α-RGCs and coupled ACs in the mouse retina.

DATA AVAILABILITY

The data that support the findings of this study are available to the corresponding author on request.

ACKNOWLEDGMENTS

We thank Dr. Stewart Bloomfield for the critical reading of the manuscript.

Present address: Q. Wang, University of Health and Rehabilitation Sciences, No. 369 Qingdao National High-Tech Industrial Development Zone, Shandong, People's Republic of China.

GRANTS

This study was supported by The Hong Kong Polytechnic University Grant UAQC, 1-WZ24 and University Research Facility in Behavioral and Systems Neuroscience. This study was also supported by the Hong Kong Research Grants Council ECS/RGC; 25103918 (to F.P.); InnoHK initiative and the Hong Kong Special Administrative Region Government. "百城百园" "专项启动基金" I2021A010; 深圳市基础研究 (面上项目) (Shenzhen Municipal Science and Technology Innovation Commission, JCYJ20210324130809025).

DISCLOSURES

No conflicts of interest, financial or otherwise, are declared by the authors.

AUTHOR CONTRIBUTIONS

F.P. conceived and designed research; Q.W., C.S., and F.P. performed experiments; Q.W., C.S., and F.P. analyzed data; Q.W., C.S., and F.P. interpreted results of experiments; Q.W., C.S., and F.P. prepared figures; Q.W., C.S., and F.P. drafted manuscript; F.P. edited and revised manuscript; F.P. approved final version of manuscript.

REFERENCES

1. **Bloomfield SA**, **Völgyi B.** The diverse functional roles and regulation of neuronal gap junctions in the retina. *Nat Rev Neurosci* 10: 495–506, 2009. doi:10.1038/nrn2636.
2. **Söhl G**, **Maxeiner S**, **Willecke K.** Expression and functions of neuronal gap junctions. *Nat Rev Neurosci* 6: 191–200, 2005. doi:10.1038/nrn1627.
3. **Peichl L.** Alpha ganglion cells in mammalian retinae: common properties, species differences, and some comments on other ganglion cells. *Vis Neurosci* 7: 155–169, 1991. doi:10.1017/s0952523800011020.
4. **Krieger B**, **Qiao M**, **Rousso DL**, **Sanes JR**, **Meister M.** Four α ganglion cell types in mouse retina: Function, structure, and molecular signatures. *PLoS One* 12: e0180091, 2017. doi:10.1371/journal.pone.0180091.
5. **Hoshi H**, **Liu WL**, **Massey SC**, **Mills SL.** ON inputs to the OFF layer: bipolar cells that break the stratification rules of the retina. *J Neurosci* 29: 8875–8883, 2009. doi:10.1523/JNEUROSCI.0912-09.2009.
6. **Gollisch T**, **Meister M.** Eye smarter than scientists believed: neural computations in circuits of the retina. *Neuron* 65: 150–164, 2010. doi:10.1016/j.neuron.2009.12.009.
7. **Baden T**, **Berens P**, **Franke K**, **Roman Rosón M**, **Bethge M**, **Euler T.** The functional diversity of retinal ganglion cells in the mouse. *Nature* 529: 345–350, 2016. doi:10.1038/nature16468.
8. **Masland RH.** The fundamental plan of the retina. *Nat Neurosci* 4: 877–886, 2001. doi:10.1038/nn0901-877.
9. **Roska B**, **Werblin F.** Vertical interactions across ten parallel, stacked representations in the mammalian retina. *Nature* 410: 583–587, 2001. doi:10.1038/35069068.
10. **Gjorgjieva J**, **Sompolinsky H**, **Meister M.** Benefits of pathway splitting in sensory coding. *J Neurosci* 34: 12127–12144, 2014. doi:10.1523/JNEUROSCI.1032-14.2014.
11. **Asari H**, **Meister M.** Divergence of visual channels in the inner retina. *Nat Neurosci* 15: 1581–1589, 2012. doi:10.1038/nn.3241.
12. **Abbott LF**, **Dayan P.** The effect of correlated variability on the accuracy of a population code. *Neural Comput* 11: 91–101, 1999. doi:10.1162/089976699300016827.

13. **Schnitzer MJ**, **Meister M.** Multineuronal firing patterns in the signal from eye to brain. *Neuron* 37: 499–511, 2003. doi:10.1016/s0896-6273(03)00004-7.
14. **Averbeck BB**, **Latham PE**, **Pouget A.** Neural correlations, population coding and computation. *Nat Rev Neurosci* 7: 358–366, 2006. doi:10.1038/nrn1888.
15. **Pillow JW**, **Shlens J**, **Paninski L**, **Sher A**, **Litke AM**, **Chichilnisky EJ**, **Simoncelli EP.** Spatio-temporal correlations and visual signalling in a complete neuronal population. *Nature* 454: 995–999, 2008. doi:10.1038/nature07140.
16. **Shlens J**, **Rieke F**, **Chichilnisky E.** Synchronized firing in the retina. *Curr Opin Neurobiol* 18: 396–402, 2008. doi:10.1016/j.conb.2008.09.010.
17. **Brivanlou IH**, **Warland DK**, **Meister M.** Mechanisms of concerted firing among retinal ganglion cells. *Neuron* 20: 527–539, 1998. doi:10.1016/s0896-6273(00)80992-7.
18. **Field GD**, **Sher A**, **Gauthier JL**, **Greschner M**, **Shlens J**, **Litke AM**, **Chichilnisky EJ.** Spatial properties and functional organization of small bistratified ganglion cells in primate retina. *J Neurosci* 27: 13261–13272, 2007. doi:10.1523/JNEUROSCI.3437-07.2007.
19. **Usrey WM**, **Reid RC.** Synchronous activity in the visual system. *Annu Rev Physiol* 61: 435–456, 1999. doi:10.1146/annurev.physiol.61.1.435.
20. **Ishikane H**, **Gangi M**, **Honda S**, **Tachibana M.** Synchronized retinal oscillations encode essential information for escape behavior in frogs. *Nat Neurosci* 8: 1087–1095, 2005. doi:10.1038/nn1497.
21. **Beaudoin DL**, **Borghuis BG**, **Demb JB.** Cellular basis for contrast gain control over the receptive field center of mammalian retinal ganglion cells. *J Neurosci* 27: 2636–2645, 2007. doi:10.1523/JNEUROSCI.4610-06.2007.
22. **Mills SL**, **Xia X-B**, **Hoshi H**, **Firth SI**, **Rice ME**, **Frishman LJ**, **Marshak DW.** Dopaminergic modulation of tracer coupling in a ganglion-amacrine cell network. *Vis Neurosci* 24: 593–608, 2007. doi:10.1017/S0952523807070575.
23. **Lakatos P**, **Gross J**, **Thut G.** A new unifying account of the roles of neuronal entrainment. *Curr Biol* 29: R890–R905, 2019. doi:10.1016/j.cub.2019.07.075.
24. **Fenno L**, **Yizhar O**, **Deisseroth K.** The development and application of optogenetics. *Annu Rev Neurosci* 34: 389–412, 2011. doi:10.1146/annurev-neuro-061010-113817.
25. **Bi A**, **Cui J**, **Ma Y-P**, **Olshevskaya E**, **Pu M**, **Dizhoor AM**, **Pan Z-H.** Ectopic expression of a microbial-type rhodopsin restores visual responses in mice with photoreceptor degeneration. *Neuron* 50: 23–33, 2006. doi:10.1016/j.neuron.2006.02.026.
26. **Pan ZH**, **Ganjawala TH**, **Lu Q**, **Ivanova E**, **Zhang Z.** ChR2 mutants at L132 and T159 with improved operational light sensitivity for vision restoration. *PLoS One* 9: e98924, 2014. doi:10.1371/journal.pone.0098924.
27. **Duan X**, **Qiao M**, **Bei F**, **Kim IJ**, **He Z**, **Sanes JR.** Subtype-specific regeneration of retinal ganglion cells following axotomy: effects of osteopontin and mTOR signaling. *Neuron* 85: 1244–1256, 2015. doi:10.1016/j.neuron.2015.02.017.
28. **Bloomfield SA**, **Miller RF.** A physiological and morphological study of the horizontal cell types of the rabbit retina. *J Comp Neurol* 208: 288–303, 1982. doi:10.1002/cne.902080306.
29. **Pan F**, **Toychiev A**, **Zhang Y**, **Atlasz T**, **Ramakrishnan H**, **Roy K**, **Völgyi B**, **Akopian A**, **Bloomfield SA.** Inhibitory masking controls the threshold sensitivity of retinal ganglion cells. *J Physiol* 594: 6679–6699, 2016. doi:10.1113/JP272267.
30. **Hu EH**, **Pan F**, **Völgyi B**, **Bloomfield SA.** Light increases the gap junctional coupling of retinal ganglion cells. *J Physiol* 588: 4145–4163, 2010. doi:10.1113/jphysiol.2010.193268.
31. **Pan F**, **Paul DL**, **Bloomfield SA**, **Völgyi B.** Connexin36 is required for gap junctional coupling of most ganglion cell subtypes in the mouse retina. *J Comp Neurol* 518: 911–927, 2010. doi:10.1002/cne.22254.
32. **Farajian R**, **Pan F**, **Akopian A**, **Völgyi B**, **Bloomfield SA.** Masked excitatory crosstalk between the ON and OFF visual pathways in the mammalian retina. *J Physiol* 589: 4473–4489, 2011. doi:10.1113/jphysiol.2011.213371.
33. **Hoshi H**, **Mills SL.** Components and properties of the G3 ganglion cell circuit in the rabbit retina. *J Comp Neurol* 513: 69–82, 2009. doi:10.1002/cne.21941.
34. **Jeon CJ**, **Strettoi E**, **Masland RH.** The major cell populations of the mouse retina. *J Neurosci* 18: 8936–8946, 1998. doi:10.1523/JNEUROSCI.18-21-08936.1998.
35. **Penn JS**, **Williams TP.** A new microspectrophotometric method for measuring absorbance of rat photoreceptors. *Vision Res* 24: 1673–1676, 1984. doi:10.1016/0042-6989(84)90325-0.
36. **Osterhout JA**, **Josten N**, **Yamada J**, **Pan F**, **Wu S-W**, **Nguyen PL**, **Panagiotakos G**, **Inoue YU**, **Egusa SF**, **Volgyi B**, **Inoue T**, **Bloomfield SA**, **Barres BA**, **Berson DM**, **Feldheim DA**, **Huberman AD.** Cadherin-6 mediates axon-target matching in a non-image-forming visual circuit. *Neuron* 71: 632–639, 2011. doi:10.1016/j.neuron.2011.07.006.
37. **Hotson JR**, **Prince DA.** A calcium-activated hyperpolarization follows repetitive firing in hippocampal neurons. *J Neurophysiol* 43: 409–419, 1980. doi:10.1152/jn.1980.43.2.409.
38. **Völgyi B**, **Pan F**, **Paul DL**, **Wang JT**, **Huberman AD**, **Bloomfield SA.** Gap junctions are essential for generating the correlated spike activity of neighboring retinal ganglion cells. *PLoS One* 8: e69426, 2013. doi:10.1371/journal.pone.0069426.
39. **Witkovsky P.** Dopamine and retinal function. *Doc Ophthalmol* 108: 17–40, 2004. doi:10.1023/b:doop.0000019487.88486.0a.
40. **Roy S**, **Field GD.** Dopaminergic modulation of retinal processing from starlight to sunlight. *J Pharmacol Sci* 140: 86–93, 2019. doi:10.1016/j.jphs.2019.03.006.
41. **Warwick RA**, **Heukamp AS**, **Riccitelli S**, **Rivlin-Etzion M.** Dopamine differentially affects retinal circuits to shape the retinal code. *J Physiol* 601: 1265–1286, 2023. doi:10.1113/JP284215.
42. **Kinane C**, **Calligaro H**, **Jandot A**, **Coutanson C**, **Haddjeri N**, **Bennis M**, **Dkhissi-Benyahya O.** Dopamine modulates the retinal clock through melanopsin-dependent regulation of cholinergic waves during development. *BMC Biol* 21: 146, 2023. doi:10.1186/s12915-023-01647-6.
43. **Zhou X**, **Pardue MT**, **Iuvone PM**, **Qu J.** Dopamine signaling and myopia development: What are the key challenges. *Prog Retin Eye Res* 61: 60–71, 2017. doi:10.1016/j.preteyeres.2017.06.003.
44. **Field GD**, **Chichilnisky EJ.** Information processing in the primate retina: circuitry and coding. *Annu Rev Neurosci* 30: 1–30, 2007. doi:10.1146/annurev.neuro.30.051606.094252.
45. **Vaney DI.** Many diverse types of retinal neurons show tracer coupling when injected with biocytin or Neurobiotin. *Neurosci Lett* 125: 187–190, 1991. doi:10.1016/0304-3940(91)90024-n.
46. **Dacey DM**, **Brace S.** A coupled network for parasol but not midget ganglion cells in the primate retina. *Vis Neurosci* 9: 279–290, 1992. doi:10.1017/s0952523800010695.
47. **Ackert JM**, **Farajian R**, **Völgyi B**, **Bloomfield SA.** GABA blockade unmasks an OFF response in ON direction selective ganglion cells in the mammalian retina. *J Physiol* 587: 4481–4495, 2009. doi:10.1113/jphysiol.2009.173344.
48. **Hu EH**, **Bloomfield SA.** Gap junctional coupling underlies the short-latency spike synchrony of retinal alpha ganglion cells. *J Neurosci* 23: 6768–6777, 2003. doi:10.1523/JNEUROSCI.23-17-06768.2003.
49. **Xin D**, **Bloomfield SA.** Tracer coupling pattern of amacrine and ganglion cells in the rabbit retina. *J Comp Neurol* 383: 512–528, 1997. doi:10.1002/(SICI)1096-9861(19970714)383:4<512::AID-CNE8>3.0.CO;2-5.
50. **Banerjee S**, **Wang Q**, **Zhao F**, **Tang G**, **So C**, **Tse D**, **To C-H**, **Feng Y**, **Zhou X**, **Pan F.** Increased Connexin36 phosphorylation in AII amacrine cell coupling of the mouse myopic retina. *Front Cell Neurosci* 14: 124, 2020. doi:10.3389/fncel.2020.00124.
51. **Yadav SC**, **Tetenborg S**, **Dedek K.** Gap junctions in A8 amacrine cells are made of connexin36 but are differently regulated than gap junctions in AII amacrine cells. *Front Mol Neurosci* 12: 99, 2019 [Erratum in Front Mol Neurosci 12: 149, 2019]. doi:10.3389/fnmol.2019.00099.
52. **Beierlein M**, **Gibson JR**, **Connors BW.** A network of electrically coupled interneurons drives synchronized inhibition in neocortex. *Nat Neurosci* 3: 904–910, 2000. doi:10.1038/78809.
53. **Veruki ML**, **Hartveit E.** AII (Rod) amacrine cells form a network of electrically coupled interneurons in the mammalian retina. *Neuron* 33: 935–946, 2002. doi:10.1016/s0896-6273(02)00609-8.
54. **Olveczky BP**, **Baccus SA**, **Meister M.** Segregation of object and background motion in the retina. *Nature* 423: 401–408, 2003. doi:10.1038/nature01652.
55. **Grimes WN**, **Zhang J**, **Tian H**, **Graydon CW**, **Hoon M**, **Rieke F**, **Diamond JS.** Complex inhibitory microcircuitry regulates retinal

signaling near visual threshold. *J Neurophysiol* 114: 341–353, 2015. doi:10.1152/jn.00017.2015.

56. **Volgyi B**, **Abrams J**, **Paul DL**, **Bloomfield SA.** Morphology and tracer coupling pattern of alpha ganglion cells in the mouse retina. *J Comp Neurol* 492: 66–77, 2005. doi:10.1002/cne.20700.
57. **Ma JSY**, **Kim JY**, **Kazane SA**, **Choi S-H**, **Yun HY**, **Kim MS**, **Rodgers DT**, **Pugh HM**, **Singer O**, **Sun SB**, **Fonslow BR**, **Kochenderfer JN**, **Wright TM**, **Schultz PG**, **Young TS**, **Kim CH**, **Cao Y.** Versatile strategy for controlling the specificity and activity of engineered T cells. *Proc Natl Acad Sci USA* 113: E450–E458, 2016. doi:10.1073/pnas.1524193113.
58. **Murphy-Baum BL**, **Taylor WR.** The synaptic and morphological basis of orientation selectivity in a polyaxonal amacrine cell of the rabbit retina. *J Neurosci* 35: 13336–13350, 2015. doi:10.1523/JNEUROSCI.1712-15.2015.
59. **Uhlhaas PJ**, **Singer W.** Neural synchrony in brain disorders: relevance for cognitive dysfunctions and pathophysiology. *Neuron* 52: 155–168, 2006. doi:10.1016/j.neuron.2006.09.020.
60. **Glass L**, **Mackey MC.** *From Clocks to Chaos: The Rhythms of Life*. Princeton, NJ: Princeton University Press, 1988.
61. **Izhikevich EM.** *Dynamical Systems in Neuroscience: The Geometry of Excitability and Bursting*. Cambridge, MA: MIT Press, 2007.
62. **Tamas G**, **Buhl EH**, **Lörincz A**, **Somogyi P.** Proximally targeted GABAergic synapses and gap junctions synchronize cortical interneurons. *Nat Neurosci* 3: 366–371, 2000. doi:10.1038/73936.
63. **Deisseroth K**, **Feng G**, **Majewska AK**, **Miesenbock G**, **Ting A**, **Schnitzer MJ.** Next-generation optical technologies for illuminating genetically targeted brain circuits. *J Neurosci* 26: 10380–10386, 2006. doi:10.1523/JNEUROSCI.3863-06.2006.